I&EC research
Industrial & Engineering Chemistry Research
pubs.acs.org/IECR
Article

# Design and Assessment of a Novel Cogeneration Process of Synthetic Natural Gas and Char via Biomass Pyrolysis-Coupled Hydrothermal Gasification

Guohui Song,* Liang Zhao, Hao Zhao, Jun Xiao, Hongyan Wang, and Shuqing Guo

Cite This: *Ind. Eng. Chem. Res.* 2020, 59, 22205−22214
Read Online



**ABSTRACT:** To simultaneously produce synthetic natural gas (SNG) and char from biomass, this paper proposed a novel cogeneration process via pyrolysis-coupled hydrothermal gasification. Two typical process configurations were designed and modeled by Aspen Plus. A mathematical model of bio-oil composition involving varieties of typical organic components was established by digging experimental data and then integrated into the Aspen Plus platform, which can describe the biomass pyrolysis process better. Taking SNG as the main product, this work focused on the effects of pyrolysis temperature, hydrothermal gasification temperature and pressure, and feedstock concentration on the composition and yield of SNG as well as energy efficiencies. The results show that the pyrolysis temperature significantly affects the yields of SNG and char, as well as energy efficiencies. Subsequently, the composition and yield of SNG are quite sensitive to the hydrothermal gasification temperature. Then, the hydrothermal gasification pressure has little influence on all process indicators. Finally, the feedstock concentration only has a small effect on $CH_4$ concentration and SNG yield. By application of the flexible operation modules of the cogeneration process, bio-oil can be potentially used as the carrier for seasonal energy storage. This cogeneration process can be regarded as a new approach to upgrade and utilize raw bio-oil.

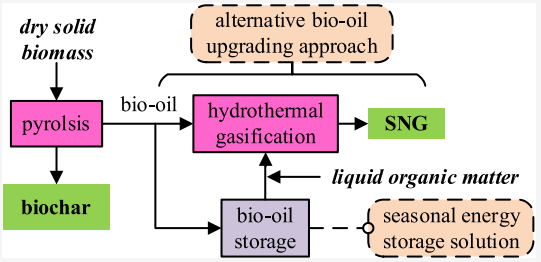


## 1. INTRODUCTION

Natural gas is a desirable clean energy resource for economic and social development, but most of the reserves are owned by a few countries, such as Russia, Iran, Qatar, the US, etc.[1] Many developing countries, e.g., China and India, suffer serious natural gas shortages. Alternatively, biomass-based synthetic natural gas (SNG) has more advantages in environmental impacts and sustainability.[2] It has certain cost competitiveness,[3] even the biomass price fluctuates within a relatively large range.[4] In this context, SNG can play an important role in reducing the natural gas gap in many countries. Additionally, there is an increasing demand for biochar in the fields such as soil remediation, contaminant adsorption, catalyst, electrochemical energy storage, mortar additive, etc.[5,6] Moreover, biochar is widely recognized as an effective material for sequestration of carbon dioxide.[6] Finally, developing a seasonal energy storage solution is also a general demand in many regions. Confronting these demands, it has important significance to investigate the SNG and biochar production technologies.

Generally and traditionally, there are three techniques of SNG production from biomass: (i) anaerobic digestion of wet biomass, (ii) gasification plus methanation of dry biomass, and (iii) hydrothermal gasification of wet biomass.[7,8] The commercialized anaerobic digestion technology has several drawbacks such as relatively low yield and energy efficiency, sensitivity to reaction temperature and pH, etc. The conventional gasification plus methanation process mainly consists of four steps in sequence: biomass gasification, syngas cleaning, methanation, and $CO_2$ removal.[9] The process has higher energy efficiencies (54−75%).[7−10] However, the process is more complex and there are some energy-intensive subprocesses and devices, e.g., the high-temperature gasification and compressors for syngas and $CO_2$. Being subject to the gasification requirement on moisture content, it is not applicable for wet biomass. The hydrothermal gasification process was developed to produce SNG from algae and manure with high conversion efficiency. It mainly comprises biomass dewatering, salt separation, hydrothermal gasification at supercritical states of water (typically 400−450 °C, 25−34 MPa), and $CO_2$ removal.[8,11] The process is relatively compact and highly efficient (>70%). However, some technical barriers such as feeding and salt separation need to be settled. It can be seen that gasification is the key step, and the type of biomass (dry or wet) is the decisive factor for the selection of suitable gasification technology. Cogasification of dry biomass and wet biomass has

Received: September 12, 2020
Revised: November 24, 2020
Accepted: December 2, 2020
Published: December 11, 2020






https://dx.doi.org/10.1021/acs.iecr.0c04504
*Ind. Eng. Chem. Res.* 2020, 59, 22205−22214

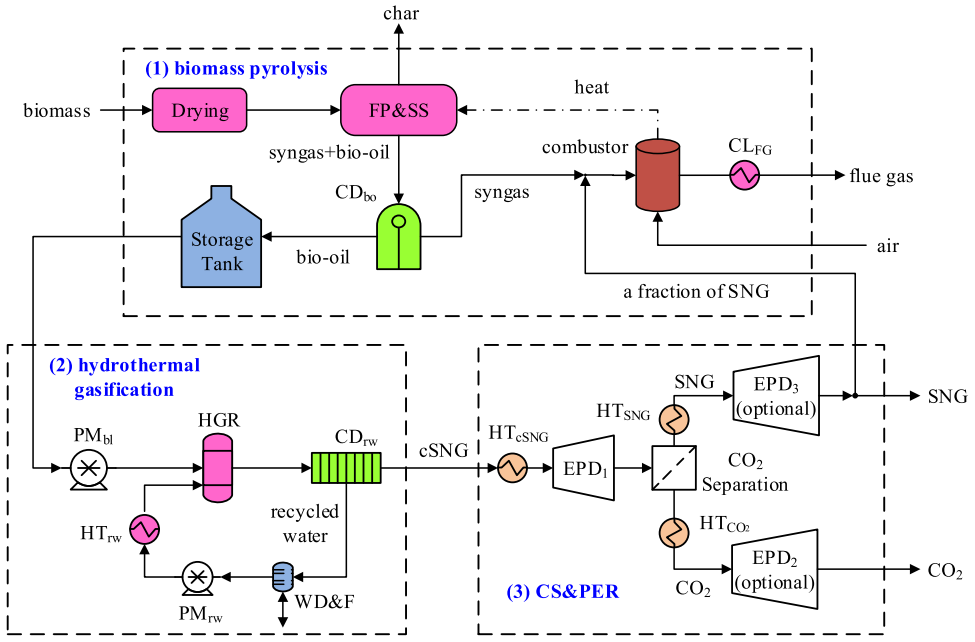


**Figure 1.** Process flow sheet of the PCHG cogeneration process.

been explored by some research studies. One treatment is to blend wet biomass with dry biomass with control of the final moisture content.[12] Alternatively, the wet biomass is dried prior to gasification by the heat generated in other steps of a biomass conversion process.[13]

With respect to biochar production, there are three mainstream techniques: (i) pyrolysis, (ii) gasification, and (iii) hydrothermal carbonization.[5,14] Pyrolysis is an efficient way to produce biochar from dry biomass, while hydrothermal carbonization can efficiently convert wet biomass. The pyrolysis platform for producing bio-oil and biochar appears to be a practical, effective, and environmentally sustainable means of producing large quantities of bioenergy and biochar.

As an efficient way to improve the conversion efficiency and usage degree of an energy resource, cogeneration offers some benefits such as increased energy efficiency, lower emissions, reduced energy costs, etc. On the one hand, the cogeneration of SNG, steam, heat and/or electricity has been extensively and deeply studied in previous works.[15−19] Recent studies showed lively interests in the cogeneration of SNG with liquid biofuels, such as methanol, dimethyl ether, etc.[20,21] On the other hand, biochar is commonly produced with bio-oil and heat, as pyrolysis is the practical and effective way for biochar production.[22] To our best knowledge, there is little investigation on cogeneration of SNG and biochar by far. Confronting the mentioned potential demands, it is meaningful to seek out a fully functional solution based on the cogeneration concept.

By re-evaluating varieties of biomass utilization methods, we found that there is a possibility to combine biomass pyrolysis and hydrothermal gasification to simultaneously solve the mentioned issues. Biomass pyrolysis is a relatively simple and inexpensive thermochemical technology for transforming biomass into bio-oil, char, and syngas.[23] Syngas can be burned to produce heat energy for various applications. Meanwhile, char can be used for a variety of purposes, such as soil remediation, waste management, greenhouse gas reduction, and building material additive.[5] As one kind of high-energy-density biofuel, bio-oil has advantages in energy storage and transportation.[24] However, bio-oil comprises a huge number of oxy-compounds and water, which vitiate its quality as biofuel. Thus, it is one of the most valued research fields to upgrade raw bio-oil against its acidity and instability. Theoretically, bio-oil can be fully converted to syngas by hydrothermal gasification at supercritical conditions, which has a robust and sufficient conversion ability.[25,26] Hence, this combination can be regarded as a new approach to upgrade and utilize raw bio-oil.

Motivated by the above demands and analyses, the objective of this work is to design a novel cogeneration process to produce SNG and char via biomass pyrolysis-coupled hydrothermal gasification, and then to carry out simulation and assessment studies on the process performances to demonstrate the technical feasibility and competitiveness.

## 2. PROCESS DESIGN

The novel cogeneration process via pyrolysis- coupled hydrothermal gasification (PCHG) was designed by combining the advantages of biomass pyrolysis and hydrothermal gasification through the connection of bio-oil. In detail, the cogeneration process mainly consists of three units (Figure 1): (1) biomass pyrolysis and bio-oil storage; (2) hydrothermal gasification; and (3) $CO_2$ separation and pressure energy recovery (CS&PER).

**2.1. Biomass Pyrolysis.** Depending on the heating rate and residence time, biomass pyrolysis can be divided into three main categories: slow, fast, and flash pyrolysis, mainly aiming at maximizing either the bio-oil or char yields.[23] In this work, we chose SNG as the main product and char as the byproduct. Hence, fast pyrolysis was integrated for the systematic process, which typically involves high heating rates (10−200 °C/s) and short residence times (0.5−10 s, typically 0.2 s). Additionally, the moisture content in biomass commonly does not exceed 15 wt %.[23] As shown in block (1) (Figure 1), the biomass pyrolysis unit mainly includes the following: a dryer, a fast pyrolysis and solid separation (FP&SS) unit, a condenser to separate bio-oil from syngas ($CD_{bo}$), and a bio-oil storage tank.

Exiting from the pyrolysis reactor, char is immediately separated from the gaseous mixture (bio-oil and syngas) at


https://dx.doi.org/10.1021/acs.iecr.0c04504
Ind. Eng. Chem. Res. 2020, 59, 22205−22214

high temperatures. As char has diverse usages with different post-treatments, no post-treatment of char was further considered in this work. The mixture is then sufficiently cooled to ambient temperature, and the liquid bio-oil is obtained and stored in the tank for the next steps.

**2.2. Hydrothermal Gasification.** As shown in block (2) (Figure 1), bio-oil at ambient pressure is first pressurized by a high-pressure bio-oil pump ($PM_{bl}$), then decomposed and reformed with supercritical water in the hydrothermal gasification reactor (HGR) with a specific catalyst,[7,8] which typically is operated in the ranges of 400−450 °C and 25−35 MPa. The syngas produced by HGR contains too much vapor, so adjacently, it is condensed by the cooler $CD_{rw}$ at high pressure to separate and recycle the water. Then, the condensed water goes through a draining and feeding device (WD&F), a water pump ($PM_{rw}$), and a water preheater ($HT_{rw}$) in sequence. The high-pressure water after preheating by the recovered heat within this process is then fed into HGR. The mass flow rate of recycled water could be adjusted by draining or feeding water. WD&F also can remove the impurities of salt.

The process is operated at supercritical conditions, where the thermophysical properties of water (such as density, viscosity, thermal conductivity, and specific heat capacity) are often orders of magnitude different with respect to subcritical conditions.[27,28] With sufficient residential time, the macromolecules in bio-oil (acids, aldehydes, ketones, phenols, etc.) can be adequately converted into the crude SNG (cSNG) via smaller molecular intermediates,[25] and the end chemical state highly depends on the methanation reactions and the water−gas shift reaction, i.e.,

$$CO + 3H_2 \leftrightarrow CH_4 + H_2O,\ \Delta H = -206\ \text{kJ/mol} \quad \text{(R1)}$$

$$CO_2 + 4H_2 \leftrightarrow CH_4 + 2H_2O,\ \Delta H = -165\ \text{kJ/mol} \quad \text{(R2)}$$

$$H_2 + CO_2 \leftrightarrow CO + H_2O,\ \Delta H = 41\ \text{kJ/mol} \quad \text{(R3)}$$

The theoretical calculation indicated that the reactor can be operated nearly isothermally without the need for efficient heat removal and heat integration.[11]

Under supercritical conditions, the solubility of minerals in water is drastically reduced, leading to precipitation and crystallization of minerals in the supercritical gasification process. This leads to agglomeration and ultimately clogging of the hydrothermal gasification.[11] Through the biomass pyrolysis step, most minerals in biomass are converted into slag and ash and then removed or filtered out. The bio-oil contains little minerals. Thus, the FP&SS unit actually plays a beneficial role in the subsequent hydrothermal gasification, which is one advantage of the cogeneration process.

Besides, there are some organic waste streams with little inorganic matter in the form of liquid, such as swill-cooked dirty oil and used oil from the automobile service industry. They could also be theoretically converted by the hydrothermal gasification process. So two feeding systems can be designed, one is for the solid biomass entering from the biomass pyrolysis unit, and the other is the liquid organic waste entering from the hydrothermal gasification unit. This is another advantage of the process regarding raw materials.

**2.3. $CO_2$ Separation and Pressure Energy Recovery.** The crude SNG obtained by the previous unit mainly contains $CH_4$ and $CO_2$. To meet the requirements of SNG, most $CO_2$ must be removed. Several mature techniques are available at present, e.g., Selexol, which can be operated at 4 bar or above.[29] The absorption pressure is kept at 4 MPa in the following study. As there is an enormous pressure difference between the hydrothermal gasification and Selexol process, the pressure energy should be utilized properly. A set of heater ($HT_{cSNG}$) and expander ($EPD_1$) are designed prior to the Selexol unit to generate electricity. In this work, the separated $CO_2$ stream is exhausted into the atmosphere, and the pressure energy of $CO_2$ is further recovered to generate electricity by another set of heater ($HT_{CO2}$) and expander ($EPD_2$) generator. The SNG is injected into an intermediate-pressure pipeline (1.6 MPa); similarly, the pressure energy is recovered by the third set of heater ($HT_{SNG}$) and expander ($EPD_3$). All of the temperatures at the outlets of the expanders are set to be around the ambient temperature by adjusting the preheating temperatures of the corresponding heaters. Finally, the SNG stream at 25 °C and 1.6 MPa is obtained.

**2.4. Systematic Energy Integration.** Except startup stage, the syngas produced by pyrolysis plus a fraction of SNG are used to provide the heat required by the fast pyrolysis reactions. To improve the systematic energy efficiency, heat energies are mainly recovered from:

(a) Cooling of pyrolysis products: a three-stage heater ($CD_{bo}$) is applied here. The pyrolysis products are first cooled to 200 °C by the first-stage heater to recover high and medium-temperature heat; then, the products are cooled to 80 °C by the second-stage heater to recover low-temperature heat. The third-stage heater is used to condensate the pyrolysis product, but the released heat is no longer included in the heat recovery.

(b) Cooling of flue gas: the flue gas is cooled to 80 °C by $CD_{FG}$ to recover plenty of sensible heat.

(c) Cooling of hydrothermal gasification reactor and products: similarly, another three-stage heater ($CD_{rw}$) is used here. The heat energy is recovered with two temperature levels (200 and 80 °C). The third-stage heater is used to condensate the vapor and no heat is recovered in this stage.

The recovered heat energies with reasonable temperature differences are preferentially provided to the heating demands within the process, e.g., biomass drying, bio-oil and recycled water preheating, and temperature adjustments prior to expanders.

As steam and electricity are the common energy carriers, excess heat energies can be converted into steam by heat exchangers or electricity by organic Rankine cycle (ORC) technology. According to the thermodynamic principles, the energy efficiency of electricity generation is much less than that of heat exchange. Hence, under the same operation conditions, the cogeneration process with steam production (CPSP) theoretically has the highest energy efficiency, while the cogeneration process with electricity generation (CPEG) has the lowest efficiency.

## 3. PROCESS MODELING AND PERFORMANCE INDICATORS

**3.1. Process Modeling.** The simulation in this work was performed using Aspen Plus, which is a powerful platform to simulate and optimize process designs.

*3.1.1. Biomass Pyrolysis Modeling.* The modeling of biomass pyrolysis was conducted based on Amutio et al.'s experimental work due to the complete and detailed data on yields and compositions of the three varieties of products (see



https://dx.doi.org/10.1021/acs.iecr.0c04504
Ind. Eng. Chem. Res. 2020, 59, 22205−22214

Table S1).[30] During pyrolysis, thousands of reactions occur simultaneously within the fraction of a minute, therefore the explanation of the precise reaction mechanism by kinetic models becomes very challenging.[31] Since bio-oil consists of a complex mixture of hundreds of organic compounds, the difficulty of pyrolysis modeling is the description of the bio-oil's composition. Thus, the modeling often requires simplification by selecting only a few components.[32]

Zhang and Kong proposed a multicomponent vaporization modeling of bio-oil using nine organic compounds as major components.[33] However, the amount of the major compounds was not sufficient for this study. Based on the Aspen platform, van Schalkwyk et al. presented a pyrolysis simulation using the mass balanced yield model.[32] They used dozens of conventional organic compounds to describe the remaining bio-oil components, of which the thermodynamic data are already available in the software. They specified unconventional components as user-defined compounds with molecular structures and assigned thermodynamic data, such as isoeugenol, lignin-derived oligomeric compounds and phenyl-coumaran compounds, cellobiose, and levoglucosan. As many studies on biomass pyrolysis only reported the amounts of some representative conventional organic substances in bio-oil, van Schalkwyk et al.'s model is unbefitting for this study as well as similar cases. Here, we tried to only use conventional organic compounds to develop a mass balanced pyrolysis model. First, we collected more typical components of bio-oil from the related literature to enlarge the numbers of bio-oil's components (see Table S2).[34−39] Then, a mathematical model (E1−E6) describing the possible compositions of bio-oil was established based on mass conservation.

For one organic molecule

$$x_{C,i} + x_{H,i} + x_{O,i} + x_{N,i} + x_{S,i} = 1 \quad \text{(E1)}$$

For bio-oil or one variety of an organic substance

$$\sum_{i=1}^{n} x_{C,i} \cdot f_i = M_C \quad \text{(E2)}$$

$$\sum_{i=1}^{n} x_{H,i} \cdot f_i = M_H \quad \text{(E3)}$$

$$\sum_{i=1}^{n} x_{O,i} \cdot f_i = M_O \quad \text{(E4)}$$

$$\sum_{i=1}^{n} x_{N,i} \cdot f_i = M_N \quad \text{(E5)}$$

$$\sum_{i=1}^{n} x_{S,i} \cdot f_i = M_S \quad \text{(E6)}$$

where $x_{C,i}$, $x_{H,i}$, $x_{O,i}$, $x_{N,i}$, and $x_{S,i}$ are the mass fractions of C, H, O, N, and S elements of the $i$th organic molecule, respectively, $f_i$ is the mass yield of the $i$th organic molecule in bio-oil,. $M_C$, $M_H$, $M_O$, $M_N$, and $M_S$ are the mass fractions of C, H, O, N, and S elements in bio-oil, respectively.

It was assumed that an approximate set of the solution could be a representative full-featured composition data of bio-oil. The trial calculation was performed until the relative error of one element's mass is within ±0.6% and the relative error of the bio-oil's mass is within ±0.01%. Then, the solution was integrated with the yield model in Aspen Plus to simulate the conversion of the biomass pyrolysis.

*3.1.2. Modeling of Hydrothermal Gasification.* Gassner et al. reported that the equilibrium conversion can be reached in experiments with given conditions at gasification temperatures around 400 °C,[40] and then the chemical reactions could be modeled by the chemical equilibrium method in the catalytic gasification step.[18] Wang et al.'s study also shows that the carbon gasification efficiency can reach a very high level.[26] The previous experimental studies showed that the crude SNG contains about 34−55 vol % $CH_4$, 40−56 vol % $CO_2$, and 3−8 vol % $H_2$, as well as <6 vol % of higher hydrocarbons such as ethane and propane.[6,10] The simulation results are as follows: 49−53 vol % $CH_4$, 34−46 vol % $CO_2$, and 5−9 vol % $H_2$, as well as <1 vol % of higher hydrocarbons. As an example, Figure 2 shows the

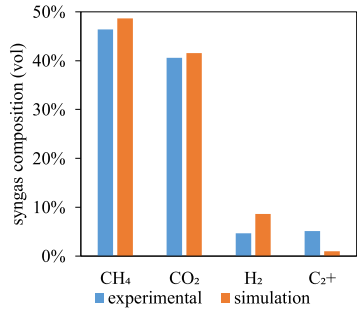


**Figure 2.** Comparison of experimental and simulation results of a case condition.

experimental and simulation results of the hydrothermal gasification of *P. tricornutum* with the feed concentration of 13 wt %.[8] The simulation results of major components are highly consistent with the experimental values, although there exist obvious differences for minor components, especially higher hydrocarbons. Together, the verification implies that the hydrothermal gasification process can be simulated by the chemical equilibrium method with the purpose of the efficiency analysis.

*3.1.3. Modeling of Other Devices.* Other devices, such as dryer, combustion unit, $CO_2$ separator, and heat exchanger and expander, are common and easy to simulate, which were modeled based on our previous studies.[17,41,42] Table 1 summarizes the key parameters for the modeling of reactors and heat exchangers. The energy efficiencies of the auxiliary devices, e.g., heat exchangers and pumps, are listed in Table 2[43,44]

**Table 1. Model Blocks and Operation Parameters of the Major Devices**

| no. | device or unit | model | parameter(s) |
|---|---|---|---|
| 1 | fast pyrolysis | Ryield | 400−600 °C, 0.1 MPa |
| 2 | $CD_{bo}$ | Heater | 200 °C/80 °C/30 °C |
| 3 | $CL_{FG}$ | Rstoic | 80 °C |
| 4 | HGR | RGibbs | 400−500 °C, 25−30 MPa |
| 5 | $CD_{rw}$ | Heater | 200 °C/80 °C/30 °C |
| 6 | $HT_{cSNG}$ | Heater | 150 °C |
| 7 | $HT_{SNG}$ | Heater | 75 °C |
| 8 | $HT_{CO2}$ | Heater | 190 °C |



https://dx.doi.org/10.1021/acs.iecr.0c04504
Ind. Eng. Chem. Res. 2020, 59, 22205−22214

**Table 2. Energy Efficiencies of Involved Auxiliary Devices**

| device | energy efficiency (%) |
|---|---|
| heat exchanger | 95 |
| pump (i) isentropic | 85 |
| (ii) mechanical | 98 |
| EPD (i) isentropic | 65 |
| (ii) mechanical | 98 |
| ORC | 25 |

**3.2. Process Indicators.** The composition and yield of SNG are key parameters to assess such a process. The SNG yield is defined as follows

$$Y_{SNG} = \frac{V_{SNG}}{m_{bm}} \quad (1)$$

where $V_{SNG}$ is the volume flow rate of SNG in $Nm^3/h$ and $m_{bm}$ is the mass flow rate of the biomass fed into the fast pyrolysis, in kg/h.

The energy efficiencies of SNG ($\eta_{SNG}$) and char ($\eta_{char}$) are defined as follows, respectively

$$\eta_{SNG} = \frac{E_{SNG}}{m_{bm}\cdot LHV_{bm}} \quad (2)$$

$$\eta_{char} = \frac{E_{char}}{m_{bm}\cdot LHV_{bm}} \quad (3)$$

The energy efficiencies of the cogeneration process with steam production ($\eta_{CPSP}$) and with electricity generation ($\eta_{CPEG}$) are defined as follows, respectively

$$\eta_{CPSP} = \frac{E_{SNG} + E_{char} + E_{heat} + E_{ele}}{m_{bm}\cdot LHV_{bm}} \quad (4)$$

$$\eta_{CPEG} = \frac{E_{SNG} + E_{char} + \sum E_{ele}}{m_{bm}\cdot LHV_{bm}} \quad (5)$$

where $E_{SNG}$ and $E_{char}$ are the energy flow rates of SNG and char, respectively, in MJ/h. The values of char's LHV are calculated and listed in Table S1. $LHV_{bm}$ is the feedstock's LHV (16.49 MJ/kg).[45] $E_{heat}$ is the energy flow rate of net recovered heat in CPSP, in MJ/h. The heat sources in the cogeneration process are as follows: high-temperature pyrolysis products, heat released during the hydrothermal gasification, and medium-temperature crude SNG. The subprocesses that consume the recovered heat are as follows: drying and preheating biomass, heating water for hydrothermal gasification, and heating cSNG, $CO_2$, and SNG before the expanders.

The simulation results show that the power consumption by pumps can be totally provided by the electricity generated by expanders in either CPSP or CPEG. Thus, $E_{ele}$ in CPSP is the net power generated by expanders, while $E_{ele}$ in CPEG is the total power generated by expanders and the ORC, in MJ/h.

## 4. RESULTS AND DISCUSSION

Taking SNG as the main product, the typical parameters are as follows: fast pyrolysis temperature ($T_{FP}$) of 500 °C, hydrothermal gasification temperature ($T_{HG}$) of 400 °C, hydrothermal gasification pressure ($p_{HG}$) of 25 MPa, and feedstock concentration ($W$) of 0.2, which is defined as follows

$$W = \frac{m_{bl,db}}{m_{bl,wb} + m_{rw}} \quad (6)$$

where $m_{bl,db}$ and $m_{bl,wb}$ are the mass flow rates of bio-oil on dry basis and wet basis, respectively, and $m_{rw}$ is the mass flow rate of water being added into the hydrothermal gasification reactor. In the following analysis of one parameter, other parameters remain unchanged.

**4.1. Effect of Fast Pyrolysis Temperature.** Table 3 shows that $T_{FP}$ has little influence on the compositions of crude SNG and SNG, as well as HHV and LHV. However, the yields of SNG and char vary significantly with $T_{FP}$. $Y_{SNG}$ reaches a maximum of 0.215 $Nm^3/kg$ at 500 °C. The reason is that the char yield decreases from 21.9 to 17.4 wt % with the increase of $T_{FP}$ (Table S1), while the bio-oil yield (wet basis) first increases from 71.2 wt % (400 °C) to 75.3 wt % (500 °C) and then decreases to 65.1 wt % (600 °C).

**Table 3. Properties of Crude SNG and SNG with Fast Pyrolysis Temperature**

| $T_{FP}$ (°C) | 400 | 450 | 500 | 600 |
|---|---|---|---|---|
| Crude SNG Composition (vol %) | | | | |
| $CH_4$ | 51.70 | 50.54 | 50.97 | 54.09 |
| $H_2$ | 2.92 | 2.86 | 2.86 | 2.78 |
| CO | 0.04 | 0.04 | 0.04 | 0.04 |
| $CO_2$ | 45.33 | 46.54 | 46.10 | 43.06 |
| $N_2$ | 0.01 | 0.02 | 0.03 | 0.03 |
| SNG Composition (vol %) | | | | |
| $CH_4$ | 90.64 | 90.42 | 90.51 | 91.38 |
| $H_2$ | 5.22 | 5.22 | 5.18 | 4.79 |
| CO | 0.08 | 0.08 | 0.08 | 0.07 |
| $CO_2$ | 4.05 | 4.25 | 4.18 | 3.71 |
| $N_2$ | 0.01 | 0.03 | 0.05 | 0.05 |
| HHV (MJ/N $m^3$) | 36.7 | 36.6 | 36.6 | 36.9 |
| LHV (MJ/N $m^3$) | 33.0 | 33.0 | 33.0 | 33.2 |
| $Y_{SNG}$ (N $m^3$/kg) | 0.117 | 0.141 | 0.215 | 0.192 |

Figure 3 shows that with the increase of $T_{FP}$, the energy efficiency of SNG ($\eta_{SNG}$) first increases from 23.2 to 42.6% and then decreases to 38.4%, which is in accordance with the variation of $Y_{SNG}$. Whereas, the energy efficiency of char ($\eta_{char}$) declines gradually from 42.4 to 29.8% as the char yield decreases with $T_{FP}$. From the systematic view, $\eta_{CPSP}$ descends gradually from 93.5 to 91.1%, while $\eta_{CPEG}$ peaks at 80.7% at 500 °C. In the case of CPSP, the heat is recovered to produce steam with very high energy efficiency (Table 2). With the rise of $T_{FG}$, the pyrolysis process generally needs more heat and consumes more SNG to provide the heat required by pyrolysis reactions. In the case of CPEG, the recovered heat is converted into electricity

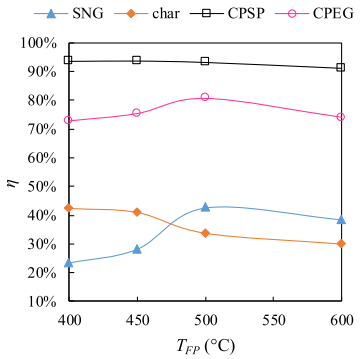


**Figure 3.** Effects of $T_{FP}$ on energy efficiencies.



https://dx.doi.org/10.1021/acs.iecr.0c04504
Ind. Eng. Chem. Res. 2020, 59, 22205−22214

with very low energy efficiency (Table 2). Figure 3 also indicates that $\eta_{CPEG}$ is determined by the sum of $\eta_{SNG}$ and $\eta_{char}$.

Taken together, $T_{FP}$ in the range of 400−600 °C has a significant influence on the process. The choice of pyrolysis temperature depends on the tendency of the ratio of SNG and char products. In this work, SNG is taken as the main product, so 500 °C is selected as a suitable pyrolysis temperature.

**4.2. Effect of Hydrothermal Gasification Temperature.** Figure 4 shows that with the increase of $T_{HG}$ from 400 to 500 °C,

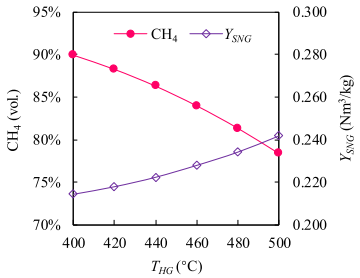


**Figure 4.** Effects of $T_{HG}$ on $CH_4$ concentration and SNG yield.

the $CH_4$ concentration decreases from 89.9 to 78.3 vol % while $Y_{SNG}$ increases from 0.214 to 0.242 $m^3$/kg. Meanwhile, HHV of SNG descends from 36.4 to 33.2 $MJ/m^3$. The reason is that higher temperature shifts the reversible reactions R1 and R2 more to the left side, which also leads to increases in the molar quantity and volume of the product.

These opposite effects together lead to a slight increase in the energy flow rate of SNG. Then, $\eta_{SNG}$ increases by about 1.2 percentage points (from 42.5 to 43.8%), which is faintly visible in Figure 5. As methanation reactions are exothermic, the

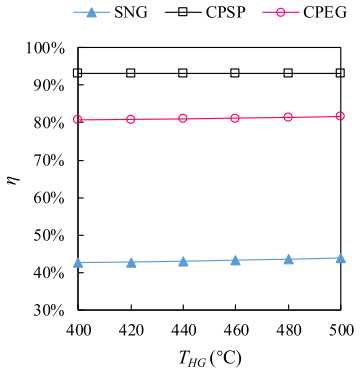


**Figure 5.** Effects of $T_{HG}$ on energy efficiencies.

recoverable heat decreases with the increase in $T_{HG}$, which would result in a slight decrease in $\eta_{CPSP}$. However, because $\eta_{SNG}$ takes account for majority of the systematic efficiencies, the small increase in $\eta_{SNG}$ counteracts the above-mentioned decrease in $\eta_{CPSP}$. Thus, $\eta_{CPSP}$ almost remains unchanged over the $T_{HG}$ range (Figure 5). As far as $\eta_{CPEG}$, the changes in recovered heat indirectly have less effect on the generated electricity by the ORC unit. Together, when $T_{HG}$ increases from 400 to 500 °C, $\eta_{CPEG}$ increases by about 1.0 percentage point (from 80.6 to 81.6%).

Additionally, the results also show that with the increase of $T_{HG}$, the $H_2$ concentration in SNG sharply increases from 5.0 to 16.6 vol % (about three times) and CO concentration also obviously ascends from 0.08 to 0.5 vol % (roughly six times), which results in a sharp decline in the quality of SNG judging by its explosion limits and toxicity.

Together, the results indicate that $T_{HG}$ is a sensitive parameter of the process and mainly affects the composition and yield of SNG. Although $CO_2$ separation efficiency in the CS&PER unit can adjust the $CH_4$ concentration in SNG, it almost has no effect on $H_2$ and CO concentrations. Therefore, the lower hydrothermal gasification temperature is positively favorable and necessary for a SNG production process at such high pressures, although it would slightly decrease the energy efficiencies.

**4.3. Effect of Hydrothermal Gasification Pressure.** Figure 6 shows that increasing $p_{HG}$ from 25 to 30 MPa leads to

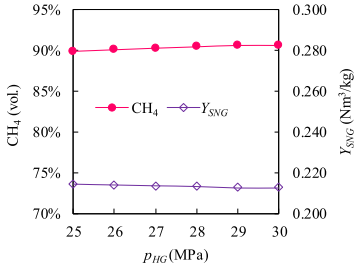


**Figure 6.** Effect of $p_{HG}$ on $CH_4$ concentration and SNG yield.

an increase in the $CH_4$ concentration from 89.9 to 90.7 vol %, while $Y_{SNG}$ decreases from 0.214 to 0.213 $m^3$/kg. Meanwhile, Figure 7 shows that the three energy efficiencies change very

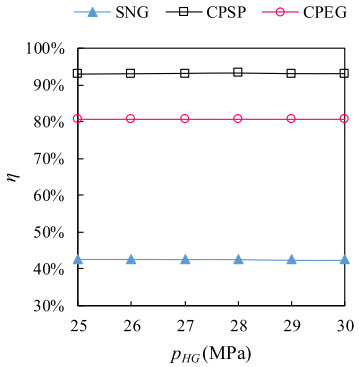


**Figure 7.** Effect of $p_{HG}$ on energy efficiencies.

little with $p_{HG}$. As all process indicators are not sensitive to hydrothermal gasification pressure, it is actually beneficial to the operation control of the pressure fluctuations.

The traditional methanation reaction of syngas was commonly carried out at 0.3−7.7 MPa with different types of methanation reactors, which can already result in a sufficient methanation extent.[9] In the case of the hydrothermal gasification process, the pressure range is quite greater than that of the traditional methanation processes, and the extra pressure has little influence on the chemical equilibrium state. It seems that the primary function of such high pressures is to maintain a supercritical state of water to enhance the decomposition and reforming of bio-oil. Thus, on the premise of the supercritical state, the lower $p_{HG}$ is preferred to reduce the cost and risk of the high-pressure reactor.

**4.4. Effect of Feedstock Concentration.** Figure 8 shows that when $W$ increases from 0.05 to 0.3, the $CH_4$ concentration in SNG gradually increases from 85.2 to 91.0 vol %, while $Y_{SNG}$ decreases from 0.225 to 0.212 $m^3$/kg. The reason is that higher


https://dx.doi.org/10.1021/acs.iecr.0c04504
Ind. Eng. Chem. Res. 2020, 59, 22205−22214

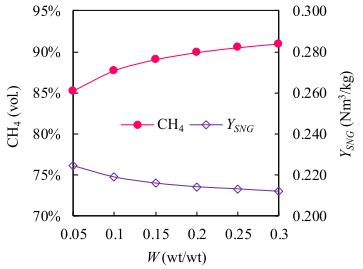


**Figure 8.** Effect of $W$ on $CH_4$ concentration and SNG yield.

feedstock concentration means less water being added into the reactor, which shifts the reversible reactions R1−R3 more to the right side. Subsequently, it leads to decreases in both molar quantity and volume of the product.

Additionally, Figure 9 indicates that with the increase of $W$, $\eta_{CPSP}$ increases visibly then slightly, by contrast, $\eta_{SNG}$ and $\eta_{CPEG}$

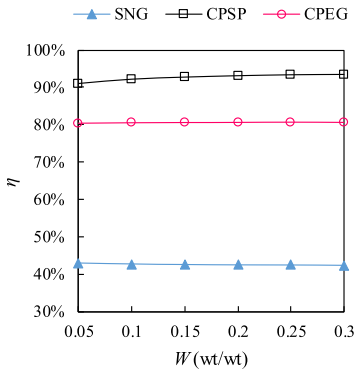


**Figure 9.** Effect of $W$ on energy efficiencies.

change a little. The main reason is that both the heat for preheating the water and the power consumed by $PM_{rw}$ decrease with the increase of $W$. On the one side, the amount of the power consumed by $PM_{rw}$ is small and has no obvious effects on the systematic efficiencies. On the other side, as a low-temperature heat stream, the change in the preheating heat for the recycled water has a visible influence on the amount of total recovered heat but little influence on that of total generated electricity. The energy efficiencies are not sensitive to feedstock concentration, which is also beneficial to operation control.

**4.5. Comparison with Other SNG Processes.** The three SNG production processes based on the thermochemical method are compared and summarized in Table 4. The analysis and comparison demonstrate that the proposed PCHG cogeneration process mainly has the following advantages:

(1) The cogeneration process is apparently quite compact as it mainly involves relatively high-density bio-oil and high-pressure gaseous streams.

(2) Two feeding systems can be designed: one is for relatively dry solid biomass, and the other is for slurry or liquid biomass with less ash, which can be pressurized by a pump.

(3) The biomass pyrolysis and product separation unit removes most inorganic matter in biomass, which can obviously reduce the difficulty and capacity of the salt removal in the hydrothermal gasification step.

(4) The PCHG cogeneration process has higher systematic energy efficiency ranges ($\eta_{CPSP}$: 91.1−93.5%; $\eta_{CPEG}$: 72.7−81.6%). It should be noticed that the formation process of char has less conversion steps and extents, as well as less energy loss according to thermodynamic principles, which contributes to such high systematic energy efficiencies. If the char is combusted with a conversion efficiency of 90% or gasified with a conversion efficiency of 80%, the systematic efficiency will at least decrease by about 3.4 or 6.8 percentage points, respectively. Additionally, the sum of the efficiencies of SNG and char is in the range of about 65−76%, which is not too high compared with the traditional processes. However, the heat recovery (as low as 80 °C, Table 1) results in an increase of 12−26% points in $\eta_{CPSP}$, which plays a crucial role in achieving such high energy efficiencies.

(5) The flexible operation modules are feasible with the design of two feeding systems and bio-oil storage (Figure 1). For example, in the period when the SNG demand is weak, one can only operate the biomass pyrolysis unit and necessary auxiliary devices, and then the bio-oil produced by this unit is fed into the oil tank for storage. By contrast, in the period when the SNG demand is strong, one can operate the whole process. Medially, one can disable the biomass pyrolysis unit and only operate the process from the hydrothermal gasification unit to the $CO_2$ separation unit.

(6) With the flexible operation modules, bio-oil, the intermediate of the PCHG process, can potentially be used as the carrier for seasonal energy storage. Whereas, in the other two processes, only biomass and LNG can be used as energy storage carriers. Here, we take the heating in winter of a town with a population of 90 000 as an example. The heating period lasts 110 days per year and the natural gas consumption is estimated to be 44.17 million $m^3$. In the case of the gasification plus methanation process, the biomass volume is approx-

**Table 4. Comparison of Three SNG Production Processes**

| SNG production process | gasification plus methanation | hydrothermal gasification | PCHG |
|---|---|---|---|
| biomass type and moisture content | most dry biomass (i.e., woody and straw biomass; $M$ <15%)[4,16,46,47] | most wet types (i.e., microalgae; $M$ > 60%)[6] | both types |
| difficulties in feeding and salt removal | low | high | low |
| SNG yield ($m^3$/kg) | 0.24−0.39 | 0.16−0.18[a] | 0.12−0.22 |
| energy efficiency | 54−75%[b] | 62−71% | 72−93% |
| energy storage carrier | dry biomass; LNG | SNG | dry biomass, LNG, bio-oil |
| technological readiness | good | R&D | concept formulated |

[a]Calculation value by this work based on $CH_4$ concentration of 90 vol %. [b]Some data were converted from energy efficiencies.



https://dx.doi.org/10.1021/acs.iecr.0c04504
Ind. Eng. Chem. Res. 2020, 59, 22205−22214

imately $267.7 \times 10^3$ $m^3$ with the assumption of the average density of 500 $kg/m^3$. In the case of the PCHG cogeneration process, the bio-oil volume is estimated to $135.9 \times 10^3$ $m^3$, which is quite smaller than that of biomass. Although the energy storage in the form of LNG has a very small volume, it requires a set of devices and consumes considerable electricity for operation. By comparison, bio-oil seems to be a better solution through empirical consideration of the volume, matching facility, and operation costs.

(7) This process can also be regarded as a new effective and simple approach of upgrading bio-oil to solve its issues such as water content, acidity, and instability.

## 5. CONCLUSIONS

This paper proposed a novel cogeneration process of SNG and char via biomass pyrolysis-coupled hydrothermal gasification. It was designed to have four functions: cogenerating both SNG and char, providing a potential seasonal energy carrier, and an alternative approach to utilize raw bio-oil. The cogeneration process has several advantages such as a compact process, ability to process both dry and wet types of biomass, low technical difficulty in the feeding system and salt removal, and higher energy efficiency as well as flexible operation modules.

To accurately simulate the biomass pyrolysis process, a mathematical model of bio-oil composition involving varieties of typical organic components was established by digging the experimental data and then integrated into the Aspen Plus platform. The modified Aspen Plus model can describe the biomass pyrolysis process better and can be referenced and migrated to other similar simulations.

The simulation results indicate that the fast pyrolysis temperature is the key parameter to adjust the product distribution (SNG and char) as well as the energy efficiencies. Hydrothermal gasification temperature is a sensitive parameter mainly affecting the composition and yield of SNG. The hydrothermal gasification pressure in the 25−30 MPa range has a little influence on all process indicators, and the feedstock concentration only has small effects on $CH_4$ concentration and yield. Thus, the process indicators are insensitive to variation in the latter two parameters, which are very beneficial to the error control in operation. Taking SNG as the main product, the optimized $T_{FP}$ and $T_{HG}$ are 500 and 400 °C, respectively, and correspondingly, the SNG yield is 0.215 $Nm^3/kg$, and the energy efficiencies of SNG, Char, CPSP, and CPEG are 42.6, 33.6, 93.1, and 80.7%, respectively.

This cogeneration process should be anticipated by the areas lacking natural gas resources. It may also be interesting to some service sectors to dispose waste oils, such as automobile oil, waste cooking oil, etc. The hydrothermal gasification is the key step of this process. As a rapid-developed conversion technology in recent years, relevant research studies have been conducted to promote its industrial application. However, there remain several key challenges of this technical route before application, such as the design of an efficient reactor, an effective and durable catalyst, high processing costs, and safety risk management. Further studies should be conducted from the above aspects.

## ■ ASSOCIATED CONTENT

### Supporting Information

The Supporting Information is available free of charge at https://pubs.acs.org/doi/10.1021/acs.iecr.0c04504.

Yields and compositions of three pyrolysis products and organic substances in the bio-oil composition model (PDF)

## ■ AUTHOR INFORMATION


### Corresponding Author

**Guohui Song** − *Jiangsu Engineering Research Center for Efficient Utilization of Regional Energy Resources, School of Energy and Power Engineering, Nanjing Institute of Technology, Nanjing, Jiangsu 211167, China; Department of Mechanical and Aerospace Engineering, Princeton University, Princeton, New Jersey 08544, United States;* orcid.org/0000-0002-2749-427X; Phone: +86-187-0516-66327; Email: ghsong@njit.edu.cn, gsong@princeton.edu

### Authors

**Liang Zhao** − *College of Materials Science and Engineering, Nanjing Forestry University, Nanjing, Jiangsu 210037, China*

**Hao Zhao** − *Department of Mechanical and Aerospace Engineering, Princeton University, Princeton, New Jersey 08544, United States; Department of Mechanical Engineering, The Hong Kong Polytechnic University, Kowloon, Hong Kong SAR, China*

**Jun Xiao** − *Key Laboratory of Energy Thermal Conversion and Control of Ministry of Education, School of Energy and Environment, Southeast University, Nanjing, Jiangsu 210096, China;* orcid.org/0000-0003-0002-2878

**Hongyan Wang** − *Jiangsu Engineering Research Center for Efficient Utilization of Regional Energy Resources, School of Energy and Power Engineering, Nanjing Institute of Technology, Nanjing, Jiangsu 211167, China*

**Shuqing Guo** − *Jiangsu Engineering Research Center for Efficient Utilization of Regional Energy Resources, School of Energy and Power Engineering, Nanjing Institute of Technology, Nanjing, Jiangsu 211167, China*

Complete contact information is available at: https://pubs.acs.org/10.1021/acs.iecr.0c04504


### Notes

The authors declare no competing financial interest.

## ■ ACKNOWLEDGMENTS

This work was financially supported by the Scientific Foundation of Nanjing Institute of Technology (YKJ201818). The first author gratefully acknowledges the financial support from the China Scholarship Council (201908320106).

## ■ NOMENCLATURE

### Abbreviations Used

| | |
|---|---|
| cSNG | crude synthetic natural gas |
| CD | condenser |
| CL | cooler |
| CPSP | cogeneration process with steam production |
| CPEG | cogeneration process with electricity generation |
| CS&PER | $CO_2$ separation and pressure energy recovery |
| EPD | expander including generator |
| FP | fast pyrolysis |
| HG | hydrothermal gasification |
| HGR | hydrothermal gasification reactor |
| HHV | higher heating value |
| HT | heater |
| LHV | lower heating value |

| | |
|---|---|
| ORC | organic Rankine cycle |
| PCHG | pyrolysis-coupled hydrothermal gasification |
| PM | pump |
| SNG | synthetic natural gas |
| SS | solid separation |
| WD&F | water draining and feeding |

## VARIABLES

| | |
|---|---|
| $f_i$ | mass yield of the $i$th organic molecule in bio-oil |
| $m$ | mass flow rate |
| $p$ | pressure |
| E | energy flow rate |
| $M_i$ | mass fractions of element $i$ in bio-oil |
| $M$ | moisture content |
| $T$ | temperature |
| $V$ | volume flow rate |
| $W$ | feedstock concentration |
| $Y$ | product yield |

## SUBSCRIPTS

| | |
|---|---|
| bm | biomass |
| bl | bio-oil |
| ele | electricity |
| db | dry basis |
| rw | recycled water |
| wb | wet basis |

## GREEK SYMBOL

| | |
|---|---|
| $\eta$ | energy efficiency |

## REFERENCES


(1) Enerdata. Global Energy Statistical Yearbook 2019. https://yearbook.enerdata.net/ (accessed Aug 2020).

(2) Feng, F.; Song, G.; Shen, L.; Xiao, J. Environmental Benefits Analysis Based on Life Cycle Assessment of Rice Straw-Based Synthetic Natural Gas in China. *Energy* **2017**, *139*, 341−349.

(3) Fendt, S.; Tremel, A.; Gaderer, M.; Spliethoff, H. The Potential of Small-Scale SNG Production from Biomass Gasification. *Biomass Convers. Biorefin.* **2012**, *2*, 275−283.

(4) Song, G.; Xiao, J.; Yu, Y.; Shen, L. A Techno-Economic Assessment of SNG Production from Agriculture Residuals in China. *Energy Sources, Part B* **2016**, *11*, 465−471.

(5) Cha, J. S.; Park, S. H.; Jung, S. C.; Ryu, C.; Jeon, J. K.; Shin, M. C.; Park, Y. K. Production and Utilization of Biochar: A Review. *J. Ind. Eng. Chem.* **2016**, *40*, 1−15.

(6) Gupta, S.; Kua, H. W.; Tan Cynthia, S. Y. Use of Biochar-Coated Polypropylene Fibers for Carbon Sequestration and Physical Improvement of Mortar. *Cem. Concr. Compos.* **2017**, *83*, 171−187.

(7) Schildhauer, T. J.; Biollaz, S. M. A. Reactors for Catalytic Methanation in the Conversion of Biomass to Synthetic Natural Gas (SNG). *CHIMIA Int. J. Chem.* **2015**, *69*, 603−607.

(8) Haiduc, A. G.; Brandenberger, M.; Suquet, S.; Vogel, F.; Bernier-Latmani, R.; Ludwig, C. SunCHem: An Integrated Process for the Hydrothermal Production of Methane from Microalgae and $CO_2$ Mitigation. *J. Appl. Phycol.* **2009**, *21*, 529−541.

(9) Kopyscinski, J.; Schildhauer, T. J.; Biollaz, S. M. A. Production of Synthetic Natural Gas (SNG) from Coal and Dry Biomass - A Technology Review from 1950 to 2009. *Fuel* **2010**, *89*, 1763−1783.

(10) Tremel, A.; Gaderer, M.; Spliethoff, H. Small-Scale Production of Synthetic Natural Gas by Allothermal Biomass Gasification. *Int. J. Energy Res.* **2013**, *37*, 1318−1330.

(11) Schildhauer, T. J.; Biollaz, S. M. A. *Synthetic Natural Gas from Coal and Dry Biomass, and Power-To-Gas Applications*; John Wiley & Sons, 2016.

(12) Ng, W. C.; You, S.; Ling, R.; Gin, K. Y. H.; Dai, Y.; Wang, C. H. Co-Gasification of Woody Biomass and Chicken Manure: Syngas Production, Biochar Reutilization, and Cost-Benefit Analysis. *Energy* **2017**, *139*, 732−742.

(13) Jia, J.; Shu, L.; Zang, G.; Xu, L.; Abudula, A.; Ge, K. Energy Analysis and Techno-Economic Assessment of a Co-Gasification of Woody Biomass and Animal Manure, Solid Oxide Fuel Cells and Micro Gas Turbine Hybrid System. *Energy* **2018**, *149*, 750−761.

(14) Li, Y.; Xing, B.; Ding, Y.; Han, X.; Wang, S. A Critical Review of the Production and Advanced Utilization of Biochar via Selective Pyrolysis of Lignocellulosic Biomass. *Bioresour. Technol.* **2020**, *312*, No. 123614.

(15) Juraščík, M.; Sues, A.; Ptasinski, K. J. Exergy Analysis of Synthetic Natural Gas Production Method from Biomass. *Energy* **2010**, *35*, 880−888.

(16) Vitasari, C. R.; Jurascik, M.; Ptasinski, K. J. Exergy Analysis of Biomass-to-Synthetic Natural Gas (SNG) Process via Indirect Gasification of Various Biomass Feedstock. *Energy* **2011**, *36*, 3825−3837.

(17) Song, G.; Feng, F.; Xiao, J.; Shen, L. Technical Assessment of Synthetic Natural Gas (SNG) Production from Agriculture Residuals. *J. Therm. Sci.* **2013**, *22*, 359−365.

(18) Mian, A.; Ensinas, A. V.; Marechal, F. Multi-Objective Optimization of SNG Production from Microalgae through Hydrothermal Gasification. *Comput. Chem. Eng.* **2015**, *76*, 170−183.

(19) Cormos, C. C. Assessment of Flexible Energy Vectors Poly-Generation Based on Coal and Biomass/Solid Wastes Co-Gasification with Carbon Capture. *Int. J. Hydrogen Energy* **2013**, *38*, 7855−7866.

(20) Arteaga-Pérez, L. E.; Gómez-Cápiro, O.; Karelovic, A.; Jiménez, R. A Modelling Approach to the Techno-Economics of Biomass-to-SNG/Methanol Systems: Standalone vs Integrated Topologies. *Chem. Eng. J.* **2016**, *286*, 663−678.

(21) Celebi, A. D.; Sharma, S.; Ensinas, A. V.; Maréchal, F. Next Generation Cogeneration System for Industry − Combined Heat and Fuel Plant Using Biomass Resources. *Chem. Eng. Sci.* **2019**, *204*, 59−75.

(22) Brynda, J.; Skoblia, S.; Pohořelý, M.; Beňo, Z.; Soukup, K.; Jeremiáš, M.; Moško, J.; Zach, B.; Trakal, L.; Šyc, M.; Svoboda, K. Wood Chips Gasification in a Fixed-Bed Multi-Stage Gasifier for Decentralized High-Efficiency CHP and Biochar Production: Long-Term Commercial Operation. *Fuel* **2020**, *281*, No. 118637.

(23) Laird, D. A.; Brown, R. C.; Amonette, J. E.; Lehmann, J. Review of the Pyrolysis Platform for Coproducing Bio-Oil and Biochar. *Biofuels, Bioprod. Biorefin.* **2009**, *3*, 547−562.

(24) Sikarwar, V. S.; Zhao, M.; Clough, P.; Yao, J.; Zhong, X.; Memon, M. Z.; Shah, N.; Anthony, E. J.; Fennell, P. S. An Overview of Advances in Biomass Gasification. *Energy Environ. Sci.* **2016**, *9*, 2939−2977.

(25) Kruse, A. Supercritical Water Gasification. *Biofuels, Bioprod. Biorefin.* **2008**, *2*, 415−437.

(26) Wang, C.; Jin, H.; Feng, H.; Wei, W.; Cao, C.; Cao, W. Study on Gasification Mechanism of Biomass Waste in Supercritical Water Based on Product Distribution. *Int. J. Hydrogen Energy* **2020**, *45*, 28051−28061.

(27) Zhao, H.; Yan, C.; Zhang, T.; Ma, G.; Souza, M. J.; Zhou, C.; Ju, Y. Studies of High-Pressure n-Butane Oxidation with $CO_2$ Dilution up to 100 atm Using a Supercritical-Pressure Jet-Stirred Reactor. *Proc. Combust. Inst.* **2020**, 1−9.

(28) Wu, Z. Q.; Ou, G. B.; Ren, Y. F.; Jin, H. Numerical Investigation on the Drag Characteristics of Supercritical Water Flow Past a Sphere. *Sci. China Technol. Sci.* **2020**, *63*, 1509−1519.

(29) Zheng, G.; Zhang, Q. Review on Biogas Upgrading Technologies for Producing Biomethane. *Trans. Chin. Soc. Agric. Eng.* **2013**, *29*, 1−8.

(30) Amutio, M.; Lopez, G.; Artetxe, M.; Elordi, G.; Olazar, M.; Bilbao, J. Influence of Temperature on Biomass Pyrolysis in a Conical Spouted Bed Reactor. *Resour., Conserv. Recycl.* **2012**, *59*, 23−31.

(31) Mishra, R. K.; Mohanty, K. Kinetic Analysis and Pyrolysis Behaviour of Waste Biomass towards Its Bioenergy Potential. *Bioresour. Technol.* **2020**, *311*, No. 123480.

(32) van Schalkwyk, D. L.; Mandegari, M.; Farzad, S.; Görgens, J. F. Techno-Economic and Environmental Analysis of Bio-Oil Production




https://dx.doi.org/10.1021/acs.iecr.0c04504
*Ind. Eng. Chem. Res.* 2020, 59, 22205−22214

from Forest Residues via Non-Catalytic and Catalytic Pyrolysis Processes. *Energy Convers. Manage.* **2020**, *213*, No. 112815.
(33) Zhang, L.; Kong, S. C. Multicomponent Vaporization Modeling of Bio-Oil and Its Mixtures with Other Fuels. *Fuel* **2012**, *95*, 471−480.
(34) Zhang, Q.; Chang, J.; Wang, T.; Xu, Y. Review of Biomass Pyrolysis Oil Properties and Upgrading Research. *Energy Convers. Manage.* **2007**, *48*, 87−92.
(35) Balat, M. An Overview of the Properties and Applications of Biomass Pyrolysis Oils. *Energy Sources, Part A* **2011**, *33*, 674−689.
(36) Wang, S.; Guo, X.; Wang, K.; Luo, Z. Influence of the Interaction of Components on the Pyrolysis Behavior of Biomass. *J. Anal. Appl. Pyrolysis* **2011**, *91*, 183−189.
(37) Onarheim, K.; Solantausta, Y.; Lehto, J. Process Simulation Development of Fast Pyrolysis of Wood Using Aspen Plus. *Energy and Fuels* **2015**, *29*, 205−217.
(38) Mohabeer, C.; Abdelouahed, L.; Marcotte, S.; Taouk, B. Comparative Analysis of Pyrolytic Liquid Products of Beech Wood, Flax Shives and Woody Biomass Components. *J. Anal. Appl. Pyrolysis* **2017**, *127*, 269−277.
(39) Li, Q.; Song, G.; Xiao, J.; Sun, T.; Yang, K. Exergy Analysis of Biomass Staged-Gasification for Hydrogen-Rich Syngas. *Int. J. Hydrogen Energy* **2019**, *44*, 2569−2579.
(40) Gassner, M.; Vogel, F.; Heyen, G.; Maréchal, F. Optimal Process Design for the Polygeneration of SNG, Power and Heat by Hydrothermal Gasification of Waste Biomass: Thermo-Economic Process Modelling and Integration. *Energy Environ. Sci.* **2011**, *4*, 1726−1741.
(41) Zhao, H.; Song, G.; Shen, L.; Yu, Y. Novel Technique Route of Coal Gasification with $CO_2$ Capture Using CaO Sorbents via Three-Stage Interconnected Fluidized Beds. *Energy Fuels* **2012**, *26*, 2934−2941.
(42) Guo, W.; Feng, F.; Song, G.; Xiao, J.; Shen, L. Simulation and Energy Performance Assessment of $CO_2$ Removal from Crude Synthetic Natural Gas via Physical Absorption Process. *J. Nat. Gas Chem.* **2012**, *21*, 633−638.
(43) Li, G.; Wu, Y.; Zhang, Y.; Zhi, R.; Wang, J.; Ma, C. Performance Study on a Single-Screw Expander for a Small-Scale Pressure Recovery System. *Energies* **2017**, *10*, 6−19.
(44) Park, B. S.; Usman, M.; Imran, M.; Pesyridis, A. Review of Organic Rankine Cycle Experimental Data Trends. *Energy Convers. Manage.* **2018**, *173*, 679−691.
(45) Sheng, C.; Azevedo, J. L. T. Estimating the Higher Heating Value of Biomass Fuels from Basic Analysis Data. *Biomass Bioenergy* **2005**, *28*, 499−507.
(46) Seemann, M. C.; Schildhauer, T. J.; Biollaz, S. M. A. Fluidized Bed Methanation of Wood-Derived Producer Gas for the Production of Synthetic Natural Gas. *Ind. Eng. Chem. Res.* **2010**, *49*, 7034−7038.
(47) Gassner, M.; Maréchal, F. Thermo-Economic Process Model for Thermochemical Production of Synthetic Natural Gas (SNG) from Lignocellulosic Biomass. *Biomass Bioenergy* **2009**, *33*, 1587−1604.



https://dx.doi.org/10.1021/acs.iecr.0c04504
*Ind. Eng. Chem. Res.* 2020, 59, 22205−22214